AD-A050 443 HUGHES RESEARCH LABS MALIBU CALIF F/G 20/5
STUDY OF SURFACE FINISHING AND COATING OF DF LASER WINDOWS.(U)
JUL 77 J A HARRINGTON, M BRAUNSTEIN, B GARCIA N00014-75-C-0891

UNCLASSIFIED NL

| OF |
AD
A050443

END
DATE
FILMED
3-78
DDC

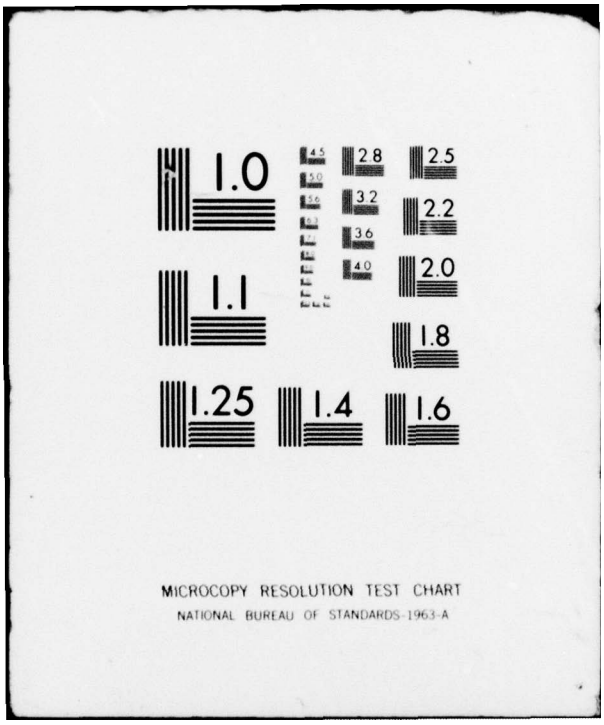
1.0
1.1
1.25
1.4
1.6
1.8
2.0
2.2
2.5
2.8
3.2
3.6
4.0
4.5
5.0
MICROCOPY RESOLUTION TEST CHART
NATIONAL BUREAU OF STANDARDS-1963-A

STUDY OF SURFACE FINISHING AND COATING OF DF LASER WINDOWS

J.A. Harrington, M. Braunstein, B. Garcia, and J.E. Rudisill

Hughes Research Laboratories
3011 Malibu Canyon Road
Malibu, CA 90265

July 1977

N00014-75-C-0891
Annual Technical Report
For Period 1 April 1976 through 31 May 1977

Sponsored By
OFFICE OF NAVAL RESEARCH
Department of the Navy
Arlington, VA 22217

UNCLASSIFIED

SECURITY CLASSIFICATION OF THIS PAGE (When Data Entered)

REPORT DOCUMENTATION PAGE		READ INSTRUCTIONS BEFORE COMPLETING FORM
1. REPORT NUMBER	2. GOVT ACCESSION NO.	3. RECIPIENT'S CATALOG NUMBER
4. TITLE (and Subtitle) Study of Surface Finishing and Coating of DF Laser Windows		5. TYPE OF REPORT & PERIOD COVERED Annual Technical Report 1 April 1976-31 May 1977 6. PERFORMING ORG. REPORT NUMBER
7. AUTHOR(s) J.A. Harrington, M. Braunstein, B. Garcia, and J.E. Rudisill		8. CONTRACT OR GRANT NUMBER(s) N00014-75-C-0891
9. PERFORMING ORGANIZATION NAME AND ADDRESS Hughes Research Laboratories 3011 Malibu Canyon Road Malibu, CA 90265		10. PROGRAM ELEMENT, PROJECT, TASK AREA & WORK UNIT NUMBERS
11. CONTROLLING OFFICE NAME AND ADDRESS Office of Naval Research Department of the Navy Arlington, VA 22217		12. REPORT DATE July 1977 13. NUMBER OF PAGES 50
14. MONITORING AGENCY NAME & ADDRESS(if different from Controlling Office)		15. SECURITY CLASS. (of this report) Unclassified 15a. DECLASSIFICATION DOWNGRADING SCHEDULE

16. DISTRIBUTION STATEMENT (of this Report)

DISTRIBUTION STATEMENT A
Approved for public release; Distribution Unlimited

(Herent from Report)

18. SUPPLEMENTARY NOTES

19. KEY WORDS (Continue on reverse side if necessary and identify by block number)
High Reflectance Mirrors, High Power DF Laser Windows, Low-Absorption Coatings

20. ABSTRACT (Continue on reverse side if necessary and identify by block number)

Research was conducted into the minimization of optical absorption in low-loss window and coating materials for use in high-power DF chemical lasers. Candidate coating materials that were investigated as single-layer, $\lambda/2$ thick films at 3.8 μm include PbF_2, ThF_4, ZnSe, Si, MgO, Al_2O_3, LiF, and NaF on CaF_2 substrates. Of these, the fluorides have the lowest absorption losses and the Si and oxide films have the

DD FORM 1 JAN 73 1473 EDITION OF 1 NOV 65 IS OBSOLETE

UNCLASSIFIED

SECURITY CLASSIFICATION OF THIS PAGE (When Data Entered)

largest. A thorough study of extrinsic absorptions in ThF_4 and ZnSe films on CaF_2 was performed in conjunction with NRL using attenuated total reflection spectroscopy. ZnSe films showed considerably less OH^- absorption than did the ThF_4 films.

TABLE OF CONTENTS

SECTION 1

INTRODUCTION

This annual report summarizes the second year of our studies on surface finishing and coating of windows for use in high-power DF laser systems. The major program goal is to conduct basic studies on the minimization of optical absorption at 3.8 μm in transparent window materials and coatings. As in the past, these studies will be coordinated with Navy needs for DF laser optical components.

The surface finishing work is concentrated on providing optimum surfaces for film adhesion and on eliminating work damage and contaminants that contribute to absorption, reduce laser damage thresholds, and reduce environmental stability. Attention is also being paid to the ability to fabricate flat and parallel windows by techniques that can ultimately be scaled up to satisfy operational needs. Emphasis is on CaF_2 since this material is currently the best candidate for the DF laser band.

The properties of the coating materials that are being studied to identify those materials that are useful in this application include refractive index, absorption and scattering in the DF laser band, compatibility with candidate DF window materials, and environmental stability. The goal is to develop a catalog of usable materials that are fully characterized with respect to optical properties, optimum preparation methods, and mechanical compatibility with the candidate window materials and with each other. Particular attention is being paid to providing for the range of refractive indices that are necessary for the design of antireflective (AR) coatings that have low reflectance over the entire DF laser band. Typical coating materials are fluorides for low refractive index, oxides for intermediate indices, and various semiconductors for high indices.

During the first year of the program, we emphasized the surveying of prospective coating materials, particularly with respect to absorption. The results indicated that existing materials can produce broadband AR coatings for fluroide windows that absorp approximately 0.05%.

During the second year, a more detailed study of coating materials was made to determine the nature of impurity absorption bands present in many common 3.8 μm coating materials. This investigation was carried out in conjunction with Drs. E. D. Palik, J. W. Gibson, R.T. Holm, and M. Hass of the Naval Research Laboratory, who carried out extensive attenuated total reflection (ATR) spectroscopy on CaF_2 samples coated in our laboratories. These collaborative efforts have resulted in several presentations at professional society meetings and in an article submitted to Applied Optics. Also during the past year, greater emphasis was placed on oxide films because of their greater resistance to environmental attack and because of their hardness.

2 TP

SECTION 2

OPTICAL ABSORPTION IN DF LASER WINDOW MATERIALS

Measurement of the absorption coefficient β is the foundation of any study of low loss materials.[1] Our calorimetric measurements of β were carried out on a wide range of candidate window and coating materials using a DF/HF chemical laser and vacuum calorimeter. The experimental setup is shown schematically in Figure 1, and the small chemical laser is shown in Figure 2. Although many different substrate hosts were studied, CaF_2 and SrF_2 were used almost exclusively for our 3.8 μm absorption studies of single-layer films and AR coatings. In general, the substrate is cleaned and then measured for the uncoated material. Next, a coating is deposited and the substrate plus film remeasured. In this way, the film absorption coefficient β_f can be extracted.

Results for the absorption coefficient β or the absorptance $A = \beta L$, where L is the sample length, are given in Table 1. The substrates were CaF_2 with a thickness of approximately 1 cm in each case, and the single-layer films had an optical thickness of $\lambda/2$ at 3.8 μm. The fluoride films exhibited the lowest absorption; the oxides and silicon had rather high absorption levels. Our work is continuing on improving the oxide films since they represent some of the best protective films available.

To improve our oxide films, a reactive evaporation procedure was established. This method consists of evaporating (using thermal sources or an E-gun) the metal in combination with a controlled amount of oxygen. An automatic pressure controller (Granville Phillips) is used to control the O_2 pressure in the evaporation chamber. Mg, Ta, and Si were used in conjunction with the O_2 to form high-quality oxide films. The best success was with Mg as the resulting MgO films have appeared the best (10^{-4} Torr pressure of O_2) of the three materials. More work is in progress to improve these methods.

---

[1] T.F. Deutsch, J. Electron. Mater. 4, 663 (1975).

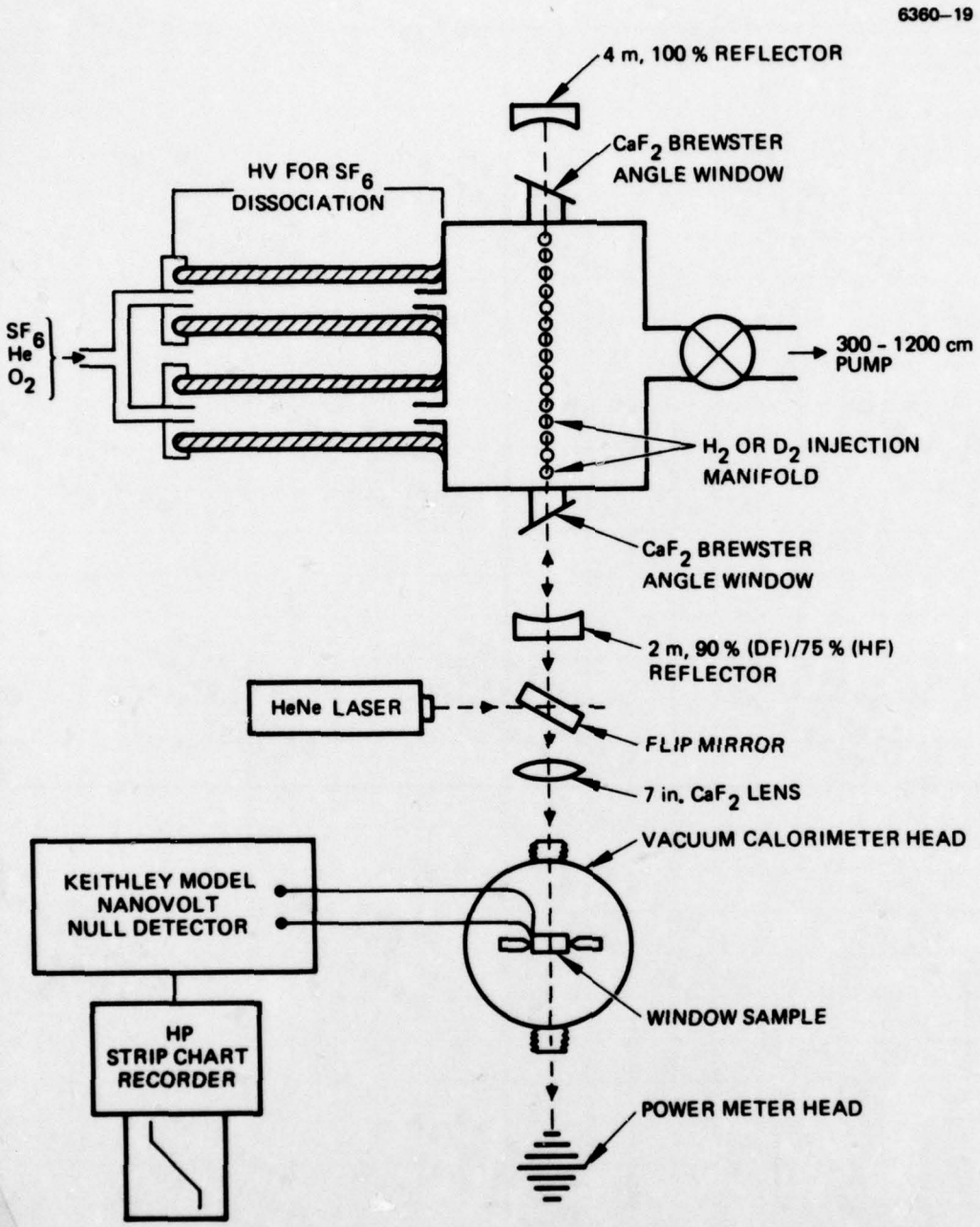

Figure 1. HF/DF laser setup.

M12171

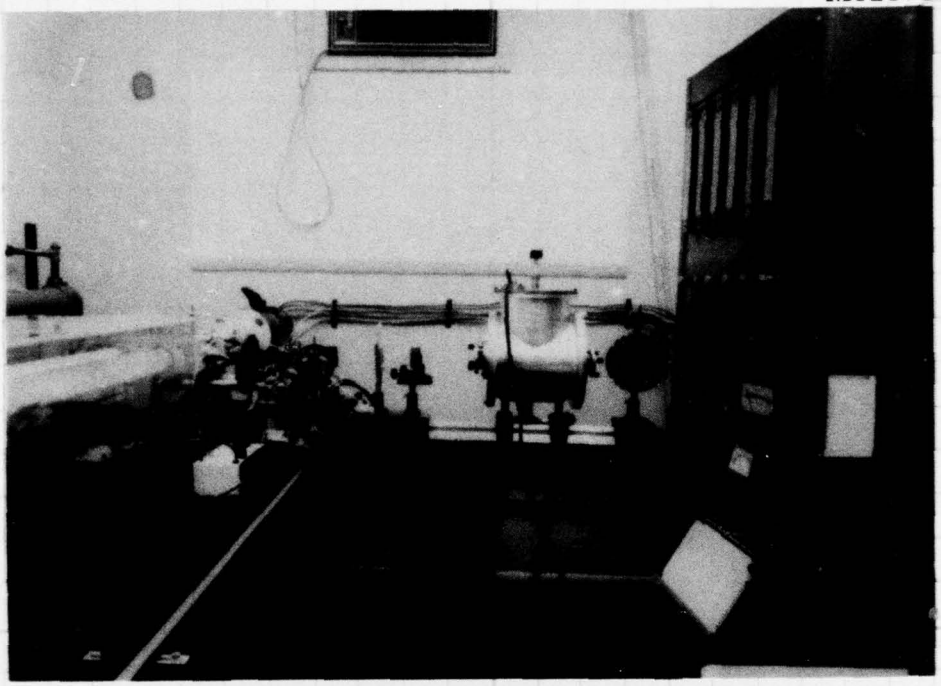

Figure 2. CW HF/DF laser facility.

TABLE 1. Single-Layer Films, $\lambda/2$ at 3.8 μm, on Both Sides of Single-Crystal CaF_2 Substrates (1.5 in. diameter by 1 cm thick)[a]

Sample No.	Coating	$A_{Uncoated}$	A_{Coated}	Absorption, %/Surface	β_f, cm^{-1}	$k_f \times 10^4$
FC-08-0	YbF_3	6.49×10^{-4}	1.77×10^{-3}	0.06	5.0[b]	1.5
FC-10-0	LiF	4.63×10^{-4}	8.24×10^{-4}	0.02	1.3	0.4
FC-6-0	PbF_2	6.11×10^{-4}	8.72×10^{-4}	0.01	1.0	0.3
FC-13-0	NaF	5.42×10^{-4}	1.36×10^{-3}	0.04	2.7	0.8
FC-22-H	Si	1.06×10^{-3}	1.98×10^{-2}	0.94	132	40
FC-13-0	Al_2O_3	5.40×10^{-4}	2.40×10^{-2}	1.17	99	30
FC-12-0	MgO	8.45×10^{-4}	1.77×10^{-2}	0.84	76	23
FC-18-H	ThF_4	6.24×10^{-4}	1.21×10^{-3}	0.03	2.5	0.8
FC-8-0	ZnSe	5.24×10^{-4}	5.60×10^{-4}			

[a]Some of these measurements were made under another complementary coating contract supported by AFML.

[b]β_f is calculated from the k_f value using $\beta_f = (4\pi k_f/\lambda)$.

SECTION 3

EVALUATION OF THIN-FILM COATINGS BY ATTENUATED TOTAL REFLECTION

To more thoroughly evaluate the extraneous absorption occurring in our thin films, a cooperative program was begun with investigators at NRL. Dr. Ed Palik, NRL coordinator, measured the near-infrared absorption from water and hydrocarbons (associated with the surfaces of CaF_2 trapezoids or with films of ThF_4 and ZnSe deposited on CaF_2 trapezoids) using ATR spectroscopy. The films deposited in our laboratory show strong absorption due to water that is probably distributed in the films for ThF_4; films of ZnSe show much less absorption.

This work is described in the Appendix, which reproduces the manuscript submitted to Applied Optics. The publications, submissions, and presentations during the year are listed below:

(1) R.T. Holm, E.D. Palik, J.W. Gibson, M. Braunstein, and B. Garcia, "Evaluation of Thin Film Coatings by Attenuated Total Reflection," presented at Topical Meeting on Optical Phenomena in Infrared Materials, Dec. 1-3, 1976, Annapolis, Maryland. Abstracts in J. Opt. Soc. Am. 67, 245 (1977).

(2) R.T. Holm, E.D. Palik, J.W. Gibson, M. Braunstein, and B. Garcia, "Attenuated Total Reflection Measurements of Absorption in Thin Film Coatings," Bull. Am. Phys. Soc. 22, 295 (1977).

(3) E.D. Palik, J.W. Gibson, R.T. Holm, M. Hass, M. Braunstein, and B. Garcia, "Infrared Characterization of Surfaces and Coatings by Internal Reflection Spectroscopy," submitted to Applied Optics.

SECTION 4

CONCLUSIONS AND PLANS

Our knowledge of low-loss window and coating materials for use at 3.8 μm has increased to the point that we can produce AR coatings that absorb 0.01% per surface. In addition, our ATR studies of impurity absorption have led us to conclude that certain materials tend to passivate and protect the surface from environmental degradation. Therefore, the thrust of our third year of effort will be toward determining the extent to which certain coating materials protect against hostile environments and whether it is possible to harden surfaces through the deposition of selective coatings.

Plans for the third year of effort include:

- AR Caoting

  Several AR coating designs will be developed for use on CaF_2 and SrF_2. Designs incorporating coating materials that are particularly resistant to attack by chemical laser or atmospheric environments will be emphasized. The optical absorption coefficient will be measured at 3.8 μm using DF chemical laser calorimetry for the coated samples.

- Environmental Studies

  Surfaces of CaF_2 samples will be exposed to environments that one would typically expect to be present in or near an operating chemical laser. The effect of surface degradation on optical absorption will be studied at 3.8 μm. The resulting effect on mechanical properties will be studied in cooperation with Dr. Roy Rice at NRL. Approximately four samples can be measured by NRL for strength and eight for delayed failure.

- Surface Hardening

Selective thin-film coatings and controlled surface finishing will be used to harden the surface of the CaF_2 substrates. The optical absorption and mechanical properties of the hardened materials will be measured as indicated above.

- Cooperation with Other Navy Programs

Close coordination and cooperation will be maintained with other workers in this area. This will include interchange of samples for evaluation, exchange of information, and coordination to maintain a cohesive effort.

APPENDIX

INFRARED CHARACTERIZATION OF SURFACES AND COATINGS BY INTERNAL-REFLECTION SPECTROSCOPY

Infrared Characterization of Surfaces and Coatings by Internal-Reflection Spectroscopy

E. D. Palik, J. W. Gibson, R. T. Holm and M. Hass
Naval Research Laboratory, Washington DC 20375
and
M. Braunstein and B. Garcia
Hughes Research Laboratories, Malibu, CA 90265

ABSTRACT

Internal-reflection spectroscopy has been used to measure near-infrared absorption due to water and hydrocarbons associated with the surfaces of CaF_2 trapezoids or with films of ThF_4 and ZnSe deposited on CaF_2 trapezoids. Films of ThF_4 show strong absorption due to water probably distributed in the film, while films of ZnSe show much less absorption which is probably primarily due to water adsorbed to the surface.

Infrared Characterization of Surfaces and Coatings by Internal-Reflection Spectroscopy

E. D. Palik, J. W. Gibson, R. T. Holm and M. Hass
Naval Research Laboratory, Washington, DC 20375
and
M. Braunstein and B. Garcia
Hughes Research Laboratories, Malibu, CA 90265

I. INTRODUCTION

Optical windows for high power cw infrared lasers should have low absorption at the operating wavelength in order to avoid heating and subsequent damage. The development of both coatings and bulk materials having low absorption coefficients has progressed substantially during the past few years, so that improvements in characterization techniques are needed.[1,2] In this present article, the following aspects concerned with low-loss optical components are discussed: (1) the characterization of low-loss surfaces and coatings by internal-reflection spectroscopy (IRS); (2) adsorption of atmospheric gases by low-loss surfaces and coatings; and (3) preparation of low-loss surfaces and coatings especially for HF/DF chemical lasers operating in the 3-4 μm region. While the discussion here is primarily concerned with anti-reflection coatings for HF/DF chemical-laser windows, the techniques presented have applications over all optical wavelength regions for thin absorbing films.

The absorption of surfaces and coatings is particularly important for current high-power lasers as the bulk absorption in many window materials has now been reduced to an extremely low level. On the other hand, surface and coating absorption can be relatively large, especially in the 3 μm and 10.6 μm regions due to H_2O, hydrocarbons and oxygen-containing impurities which may arise from atmospheric sources or are difficult to remove from coating materials.

The absorption of low-loss optical surfaces and coatings can be measured in a number of ways; laser calorimetry and internal-reflection

spectroscopy are often employed. Here, laser calorimetry is useful because of its sensitivity, simplicity, and ability to accommodate different geometrical sample shapes. However, this technique is limited to wavelengths where strong laser sources are available. IRS has received limited use in coating characterization, although it is potentially very valuable.[1-5] While IRS samples are restricted to specially prepared trapezoids, the complete infrared spectrum can be obtained using commercially available apparatus with moderately high sensitivity. Thus, the absorbing bands associated with molecular impurities, believed to cause much of the extrinsic absorption in coatings, can be identified. While the extraction of absorption coefficients from the experimental results is not simple, methods of analysis presented previously by two of us[6] indicate a systematic procedure for accomplishing this.

The use of IRS to study laser-window surfaces was introduced by Deutsch[2] who found absorption bands identified with H_2O, hydrocarbons, and oxygen-containing impurities in alkali halides and alkaline-earth fluorides. This work was extended to consider coating materials such as ThF_4 and ZnSe by Willingham, et al.[5] This work showed that H_2O impurities in or on coatings could be revealed by internal-reflection spectroscopy. However, the extraction of absorption coefficients from internal-reflection spectroscopy data was not attempted by these workers. While IRS has been widely employed over the past decade, most work in this area has been limited to the study of higher absorbing films with low indices of refraction on high-index substrates in the thin- and thick-film limits. A general treatment of low absorbing films having indices of refraction higher than or lower than that of the substrate has not been utilized to the best of our knowledge.

In this present article, the preparation and characterization of low-absorbing films of ThF_4 and ZnSe are discussed in detail. Here, ThF_4 can serve as the low-index component and ZnSe as a high-index component of a multilayer antireflection coating. The internal-reflection spectra of these coating materials on CaF_2 substrates have been obtained, and qualitative information concerning absorbing impurities in these films can be deduced. Estimates of the absorption

coefficients of these coating materials have been obtained using considerations presented previously.[6] Some guesses as to the location of the impurities (on the surface of the film or incorporated in the film) are made. Both the uncoated CaF_2 surface and the film surface can pick up impurities (presumably during the evaporation process or from the laboratory air), some of which can be identified as water and hydrocarbons from the spectra. The return of hydrocarbons and water to clean surfaces has been studied over a period of hundreds of hours.

II. EXPERIMENTAL PROCEDURES

A. Optical techniques

We have used the phenomenon of attenuated total reflection (ATR) to reveal the absorption bands of a thin film on the parallel surfaces of a CaF_2 trapezoid. In most cases spectra were recorded with a Perkin-Elmer Model 521 double-beam spectrometer. Commercial IRS single- and double-pass attachments were used. It often helped to use s- and p-polarized light in these experiments, since calculated ATR spectra show dramatic differences in polarization intensities as a function of frequency, film thickness, and angle of incidence.[3,6] We were able to place an uncoated reference trapezoid into the reference beam as a standard to record the ratio spectrum. However, we usually did not do this because the amount of water adsorbed on the double-pass CaF_2 reference trapezoid always gave 6-7% peak absorptance near 3400 cm^{-1}, while the absorptance due to the water on or in the film was much less for ZnSe and much more for ThF_4. We found it easier to record the spectra with the sample in the sample-beam attachment and a mirror replacing the entrance face of the trapezoid in the reference-beam attachment. Then in the spectrum we estimated where the background level would be if the trapezoid and film had no absorption bands. Using two attachments did, however, make the path lengths in the reference and sample beams nearly equal, thus minimizing the effects of atmospheric absorption of water and carbon dioxide.

B. Analytical techniques

Much of the previous work utilizing ATR was analyzed using the effective-thickness concept in the thin- and thick-film approximation.[3]

Our analysis of absorption in a thin film on a trapezoid utilizes the multiple-layer calculations of Wolter.[7] The pertinent result is based on the general expression for reflectance R for a three-layer system containing the substrate trapezoid, a film, and air:[6]

$$r = r^* r$$

$$r = \frac{(g_t - g_f)(g_f + g_a) + (g_t + g_f)(g_f - g_a)\, e^{i\theta}}{(g_t + g_f)(g_f + g_a) + (g_t - g_f)(g_f - g_a)\, e^{i\theta}} \tag{1}$$

with

$$\phi = 4\,\pi\omega d(n_f^2 - n_t^2 \sin^2 \theta_t)^{1/2} \quad ,$$

where ω is the frequency of the light in cm^{-1}, d is the film thickness in cm, and θ_t is the angle of incidence in the trapezoid. The subscripts t, f, and a denote trapezoid, film and air, respectively. For s polarization

$$g_j = (n_j^2 - n_t^2 \sin^2 \quad _t)^{1/2} \quad , \; j = t, f, a, \tag{2}$$

while for p polarization, the same function is divided by n_j^2. Only the refractive index n_f is assumed complex, since we anticipate absorption in the film. The internal reflectance loss per reflection for s or p polarization is termed the absorptance A defined by

$$A \equiv 1 - R \; . \tag{3}$$

Then for N internal reflections the s- or p-polarized total absorptance is

$$A_N = 1 - R^N \quad . \tag{4}$$

To estimate the peak absorption coefficient for an experimentally observed line (due to water in the film, for example), the known parameters of the trapezoid and film are used, while the imaginary part of the complex index of refraction $n_f = n + ik$ is treated as an adjustable parameter. The calculation is performed until a value of extinction coefficient k is found that accounts for the absorption seen in the spectrum. The intensity absorption coefficient α is given by

$$\alpha = \frac{4\pi\omega}{k} \quad . \tag{5}$$

We are assuming that the oscillator producing the absorption line is very weak and makes a negligible contribution to the background

index of refraction of the film material. This is reasonable in view of the fact that the peak α will typically be much less than 500 cm^{-1}. Generally, we measure peak absorption of broad or narrow lines with adequate instrumental resolution, so that we need not consider integrated absorption.

C. Trapezoids

A typical trapezoid is illustrated in Figure 1. It was nominally 5 cm long, 2 cm wide, and 0.18 cm thick. The angles at the base ends of the trapezoid were $\theta_1 = 48^o$ and $\theta_2 = 56.5^o$. These angles were chosen to allow the trapezoid to be either double-passed (by placing a mirror surface against the θ_2 surface) or single-passed (without the mirror). The double-passed trapezoid provided 38 surface reflections (25 down and 13 back), one reflection at the θ_2 face, and two transmissions at the θ_1 face. The internal angle of incidence for the down pass was $\theta_t = 48^o$; the return-pass angle of incidence was 65^o. For a single pass, there were 25 surface reflections and two transmissions at the θ_1 and θ_2 faces. Since the end faces were not coated, there was no absorption at these surfaces. However, for measuring adsorption of H_2O and CH on uncoated, clean surfaces, the effects of these end faces should be considered. Two to three transmissions are equivalent to one reflection, because of effective-thickness considerations.[3]

Paths of an IR beam in a trapezoid for single and double passes are shown in Figure 1. Even though $\theta_1 \neq \theta_2$ (a requirement for double passing), it is quite easy to use the trapezoid in the single-pass configuration in a commercial attachment. The graphical analysis for single or double passing is illustrated by the "fold out" trapezoids, which makes it simpler to visualize the beam.

A ray incident normal to the entrance face is multiply reflected to the other end of the trapezoid where, for single passing, it exits and for double passing, it is reflected and returned to the entrance face. θ_1 is the angle of incidence for the ray at each internal reflection until the end face is reached. After reflection from the second end face, the angle of incidence at each internal reflection of the return ray is $2\theta_2 - \theta_1$. These internal reflection angles must be large enough to ensure total reflection for this multi-layer system.

The return ray strikes the entrance face at an angle of incidence of $2(\theta_2 - \theta_1)$ and is refracted out of the trapezoid at an angle $\phi = \sin^{-1}[n_t \sin 2(\theta_2 - \theta_1)]$. For some commercial ATR attachments this angle is fixed at 24^o. In that case $(\theta_2 - \theta_1)$ will equal $1/2 \sin^{-1}[\sin 24^o/n_t]$. Trapezoid angles θ_1 and θ_2 are chosen to satisfy this relation for double passing. It is interesting to note that this low-index trapezoid cannot be used for double passing in the reverse direction, for when the ray is incident normal to the $\theta_2 = 565^o$ face, on the return pass, the angle of incidence is less than critical.

As shown in Figure 1, the ray will be reflected $m = (\ell/w)\cot\theta_1$ times on the down pass. Here, ℓ is the median length of the trapezoid and w is the thickness. Necessarily, m is an odd number. On the return pass the number of internal reflection is $m' = (\ell/w)\cot(2\theta_2 - \theta_1)$, where m' must also be an odd number.

Figure 1 shows the case in which a single ray enters the center of the entrance face, is reflected at the center of the second face, and is again refracted out at the center of the entrance face. This will only occur for particular values of the length, thickness and trapezoid angles. Because $\theta_1 \neq \theta_2$, all rays entering the trapezoid do not necessarily hit the same face; some are reflected off adjacent faces to be diverted out of the main beam. Since there is significant beam divergence in an optical system, the actual intensity of the exiting beam is not a severe function of the trapezoid length.

D. Film-deposition procedures

Antireflection coatings can range from simple one-layer coatings to multilayer stacks consisting of films of various indices of refraction.[8] Single layers, although simplest in design, must have a refractive index equal to the square root of the substrate index. To achieve greater flexibility in choice of materials, two-layer systems consisting of alternate high- and low-index materials have been employed, especially for high power infrared optics, where absorption in the films makes it desirable to reduce the number of layers to a minimum.[9] The choice of particular coating materials depends upon a number of factors including bulk- and film-absorption coefficients, quality of deposited film, damage resistance, hardness, and degree of

pickup of water from atmosphere. In the 10.6 μm region, previous work[9] has shown that ThF_4 provides superior properties as the low-index film, and that ZnSe provides a high-quality, high-index film. Consequently, these materials were selected for the work presented here for coatings suitable for the 3-4 μm region. However, other materials such as PbF_2 could also be used as the low-index material in the 3-5 μm region. ZnS and As_2S_3 have been successfully employed as high-index coatings for infrared optics and have some advantages for certain situations.

Previous work[10] has shown that the best films were produced using high quality starting materials under carefully controlled conditions. Here, best results for ThF_4 were obtained using starting material from Cerac, Inc., which had a 10.6 μm absorption coefficient of about 12 cm^{-1}. Most of the films were prepared using this starting material with one film made from ThF_4 purified at Hughes Research Laboratories having an absorption coefficient of 6 cm^{-1} at 10.6 μm. For ZnSe, material from Raytheon Corp., prepared by controlled vapor deposition (CVD), was employed having a bulk absorption coefficient of about 0.8 cm^{-1} at 10.6 μm.

In addition to the use of high-quality starting materials, careful substrate cleaning and use of heated substrates during evaporation were found to lead to better adhesion, higher damage resistance, and lower film absorption. Best results have been obtained by first soaking the substrate in detergent (Decontam) for about 15 minutes, followed by washing in distilled water and alcohol. The substrate was then placed in a Freon degreaser and moved to the vacuum chamber while warm. The vacuum system was pumped down and a glow discharge of 20-30 minutes applied before deposition. Substrate temperatures of about 200°C were adequate to produce films having low absorption without breakage of the fragile trapezoids.

The trapezoid holder was designed so that the two end faces were masked and thus not coated. To cover both sides of the trapezoid with films, it was necessary to break vacuum after one film was deposited, rotate the trapezoid 180° and then pump down again. Reflectance optical monitoring was used to control the film thickness. Sometimes

a mechanical stylus was used to determine the film thickness of a reference film deposited at the same time. Table 1 summarizes the pertinent deposition information. For calculational purposes we have assumed the near IR indicies of refraction of CaF_2, ThF_4, and ZnSe to be 1.41, 1.45 and 2.42, respectively.

III. EXPERIMENTAL RESULTS

A. Uncoated trapezoids

Before films were deposited and studied, it was necessary to understand the ATR spectrum of the CaF_2 trapezoid itself. Prominent H_2O and CH bands were always present on trapezoids as received from the vendor. A typical spectrum is shown in Figure 2. The standard polish gave an "orange peel" surface which produced scattering, thus causing the downhill slope toward the visible region of the spectrum. Further polishing to eliminate this roughness made the ATR essentially horizontal as indicated by the dash-dot line. We have omitted the absorption bands due to H_2O and CH here. Trapezoids of most materials we have looked at (including CaF_2, Si and GaAs) always showed the CH bands strongly (at least a few percent absorptance); the H_2O band was strong in CaF_2 and weak in the other trapezoids. When the CH absorption near 2920 cm^{-1} was strong, a band appeared at 1733 cm^{-1}, which was probably CH related. The water band at 1620 cm^{-1} (indicated by the arrow) was not observed in the present spectrum,[11] but a structure was seen near 1550 cm^{-1} which appeared on all the CaF_2 samples, generally with weaker intensity than shown in Figure 2. This feature is not in some of the spectra of Deutsch and Rudko,[2,4] who also studied uncoated CaF_2 trapezoids. Absorptance is determined by dividing the ordinate at the center of the absorption band by the ordinate of the estimated background level. We assume that since all trapezoids were mechanically polished with standard polishing compounds, such as Linde A or equivalent, that the surfaces were damaged to a depth of many hundreds of Angstroms.[12] The large surface of the trapezoids was a [III] surface, as determined from X-ray orientation, but we must assume a polycrystalline surface region due to the polishing damage. Also, this region probably has more surface area than an undamaged surface.

We cleaned the surface of CaF_2 in three ways: trichloroethylene degreaser, RF glow discharge in air or argon, and vacuum baking at 300° to 400°C for up to 3 hours. These methods are simpler than the cleaning methods used prior to coating. After cleaning, the trapezoid had to be carried to the spectrometer in air, and spectra were obtained about 15 minutes after cleaning. In all trapezoids the H_2O band was essentially unchanged, while the CH bands were almost absent (typically the total absorptance was < 0.5% on double-pass trapezoids). We noticed, however, that after a period of hours, the CH bands had grown in intensity. During this time the trapezoids were kept in laboratory air clamped in a delrin holder either touching the delrin plastic or separated from it by aluminum foil which itself had been plasma cleaned. The reappearance of CH absorption was monitored at the peak of the 2920 cm^{-1} band and is indicated in Figure 3 as percent absorptance for double-passing vs time. This was done for three materials, CaF_2, Si and ThF_4-coated CaF_2 (C in Table 1).

The increase of absorption was very rapid for all three surfaces initially. The absorption of the CH on CaF_2 tends to saturate after several days. While not shown here, absorptance in another CaF_2 sample saturated just over 9.0% at 355 hours. The absorptance for Si tended to saturate near 6.0%. The absorptance due to CH returning to the surface of a ThF_4 film on a CaF_2 trapezoid (C) was somewhat different. Saturation was apparently reached at 4.1% within three days. Then the absorptance began to rise again, and a point at 10.5% (not shown) was obtained after 449 hours. For the CaF_2 and Si samples there is a rapid initial growth in absorption taking place in a few hours and then a slower growth taking days until saturation is reached. We have fitted this slow growth region with the formula

$$A = A_o + A_1 (1 - e^{-t/\tau}) , \qquad (6)$$

where A_o crudely takes account of the initial rapid rise. The fits are given by the solid lines through the CaF_2 and Si data points. For CaF_2 we find $A_o = 1.0$, $A_1 = 8.0$ and $\tau = 110$ hr; for Si we find $A_o = 1.7$,

$A_1 = 4.3$ and $\tau = 130$ hr. Since the uncertainty in A was typically $\pm$ 0.4 percentage units on the ordinate of Figure 3, the fits for CaF_2 and Si are reasonable for t > 10 hours. We note that the values of A_o and τ are comparable for CaF_2 and Si. The initial rapid rise may be due to a fast chemisorption building up to a monolayer and then a slow physisorption which takes days to reach saturation. For ThF_4 we fitted the data for t < 100 hours with $A_o = 1.8$, $A_1 = 2.3$ and $\tau = 8$ hr. There are meager data for ThF_4, so the initial rapid rise in absorptance is not so apparent. The saturation is evident, however. The time constant for this process is much faster than for CaF_2 and Si. The additional growth beyond 100 hr is not understood but could be due to a change in the CH content of the laboratory air.

The Si trapezoid had $\theta_1 = 45^o$ and $\theta_2 = 48^o$ with $\ell = 5.1$ cm and w = 0.1 cm. The down pass produced 51 reflections while the return pass produced 41 reflections. For both kinds of trapezoids (Si and CaF_2), the absorptance per surface down and back are different because the angles are different. However, for Si the differences are small and to a good approximation the absorptance per surface at the saturation level of Figure 3 is 6.0/92 = 0.06%. A crude estimate of the saturated absorption per surface for CaF_2 is 9.0/38 = 0.24%. However, in practice one must take into account both the polarizations and angles to obtain a more precise value of absorptance per surface. The level of absorptance at saturation for a CaF_2 surface is about four times more than for a Si surface. This difference is due primarily to the effective thickness factor,[3] which is a function of the indices of refraction of film and trapezoid. This indicates (as will be shown shortly) that the actual CH films on each material are about the same thickness. This seems reasonable, since after the formation of the first monolayer or two, any further adsorption of CH should not depend on the substrate material, although it may depend on the orientation of the molecules in the first monolayer.

Since many hydrocarbons possess these characteristics, three absorption bands in the same spectral region, we cannot identify the specific chemical compound, and we can only estimate the thickness of

the layer. For example, polyethylene has these three bands with the peak absorption coefficient of the center band being 3000 cm^{-1} and the index of refraction being 1.5. Therefore, we have computed the ATR effect expected for a polyethylene layer on CaF_2 for one reflection for s- and p-polarized light with $\theta_t = 48^o$ (dashed curves) and $\theta_t = 65^o$ (solid curves). To do this we have used Eqs. 1 and 2. The results are given in Figure 4. The absorption in s polarization is stronger than the absorption in p polarization for each angle.

For the single-pass trapezoid we can calculate the total absorptance at $\theta = 48^o$ and N = 25 for each polarization from

$$A_{T(s,p)}(\theta,N) = 1 - R_{s,p}(\theta)^N \simeq N[1 - R_{s,p}(\theta)] \qquad (7)$$

and the unpolarized absorptance from the average of these two quantities. For the double-pass trapezoid the total absorptance for s and p polarization is obtained from

$$A_{T(s-p)}(\theta) = 1 - R_{s-p}(\theta) \quad , \qquad (8)$$

where

$$R_{s-p} = [R_s(48^o)^{25}R_s(65^o)^{13} + R_p(48^o)^{25}R_p(65^o)^{13}]/2 \quad . \qquad (9)$$

The right ordinates in Figure 4 can be used to obtain the various values of R needed in Eq. 9.

We measured the polarization of the CH bands after the saturation of Figure 3 was achieved on double-pass trapezoids. The results given in Figure 6a show polarization slightly stronger than p polarization. We also measured the polarization properties of these bands for a CaF_2 trapezoid as received from the vendor; the results are shown in Figure 5b. In this case, the peak absorption for a "dirty" surface was very strong. The experimental s- and p-polarization effects were in agreement with the calculation for a polyethylene film. Even though the total absorptance of CH on CaF_2 and Si are significantly different, the thickness of polyethylene required to give these absorptances is nearly the same. A detailed calculation indicates the saturated absorptance in Figure 3 for CaF_2 is equivalent to a sheet of polyethylene about 21 Å thick. For Si it is equivalent to a sheet of polyethylene about 17 Å thick. Absorptance for the "dirty" surface of CaF_2 in Figure 5b is equivalent to a sheet of

polyethylene about 100 Å thick. Interestingly, fingerprints left on the trapezoid show these same three bands. These absorption experiments graphically indicate why it is routine in ultra-high vacuum (UHV) procedures to expose the surfaces to air for a minimum time, so as to reduce hydrocarbon contamination.

The water band was always present after cleaning the trapezoid and transporting it to the spectrometer in laboratory air. This peak percent absorptance was always 6.5% ± 0.4% in numerous double-pass trapezoids for unpolarized light, and was proportionally smaller in single-pass trapezoids. We can estimate the thickness of a water film necessary to produce this absorptance by using the optical constants of water[13] and calculating curves similar to Figure 4. The optical constants of ice might be more appropriate since, presumably, the molecules do bond to each other. Such a calculation (Figure 6) using Eqs. 1 and 2 indicates that a water film of about 4 Å thickness would be needed to produce 6.5% absorptance. The average (unpolarized) total absorptance per surface for 48^{o} and 65^{o} can be determined from measurements of single- and double-passed trapezoids. For small absorption, the total absorptance as given by Eqs. 8 and 9 simplifies to the sum of the four individual absorptances of Eq. 7 divided by two. A 4 Å water film gives $A_{Ts}(48^{o},25) = 0.062$, $A_{Tp}(48^{o},25) = 0.036$, $A_{Ts}(65^{o},13) = 0.021$ and $A_{Tp}(65^{o},13) = 0.015$. We experimentally measured the ATR of a single-passed trapezoid with unpolarized light and obtained $A(48^{o},25) = 0.047$ in good agreement with the calculated result of 0.049. But measured s- and p-polarized spectra indicate that p absorption is slightly larger than s absorption, contrary to the specific calculated results of Figure 7, so our estimates of water-film thickness and absorptance per surface must be tentative. Also, it is not clear that the bulk optical constants are applicable for a one or two monolayer film.

However, in other experiments, Gibson, et al.[14] have placed a CaF_2 trapezoid into a UHV chamber, cleaned the surface by vacuum baking and determined that the surface was free of water absorption. Then, upon introducing distilled water into the chamber, they have

observed a very rapid return of water absorption. This "water" film consisted of a thin chemisorbed layer ~3Å thick and a thicker physisorbed layer ~10Å thick at saturated vapor pressure.[11] The latter could be removed by vacuum pumping, the former only by vacuum baking. These water films obeyed the polarization rules of Figure 6 at 3400 cm^{-1}, i.e., s absorption greater than p absorption. This is contrary to the polarization observed for water films formed when air was introduced into the vacuum system. This reversal in s- and p-polarization absorption can be understood in terms of a slight change in index of refraction of the film. Note that this total film is much thicker than the film formed in air at roughly 50% relative humidity. We conclude that while plasma cleaning and vacuum baking may remove water from the surface, it returns immediately when the surface is exposed to air. Also, the optical properties of the water film depend on whether it forms from pure water vapor or from air conditioning water vapor.

The total absorptance per surface of water on CaF_2 which we see for $\theta_t = 48^o$ is 0.19% for unpolarized radiation at 3400 cm^{-1}. This value depends on the internal angle of incidence. Because the average effective thickness is ~4.3d, normal-incidence absorptance in the film would be 0.044% when measured in transmission. It is this number which should be compared to a laser-calorimetry value. Laser calorimetry on CaF_2 surfaces has been done with HF lines in a band around 3600 cm^{-1}, and values vary considerably - 0.03%[15], 0.1%[16] and 0.05%.[17] Since the absorption coefficient of water is about a factor of 3 smaller at 3600 cm^{-1} than it is at 3400 cm^{-1}, our number, corrected for this is 0.015%, which is somewhat smaller than the calorimetry values. However, the ATR tends to confirm that water is the surface absorber.

Kraatz and Holmes[18] have measured the total absorptance of CaF_2 at DF and CO laser wavelengths. While they did not separate surface and bulk absorption, they did note differences for various crystal orientations which implies that surface absorptance may be different on various crystal surfaces.

B. ThF_4/CaF_2

The unpolarized ATR spectra of two CaF_2 double-pass trapezoids, C and G, coated on both sides with a layer of ThF_4 are shown in Figure 7. Pertinent parameters for these films are found in Table 1. Several features of the C spectrum are worth noting. The sharp band at 3660 cm^{-1} is probably due to the vibration of an OH group.[19] The broad band centered at 3400 cm^{-1} is no doubt due to H_2O. The three bands near 2920 cm^{-1} are due to CH at the surface. The band at 1620 cm^{-1} may be due to H_2O, since the angle-bending mode of adsorbed water had been observed at this frequency.[12] There should be a correlation between the intensities of this band and the symmetric and anti-symmetric bond-stretching modes occurring near 3400 cm^{-1}. Another band at 2225 cm^{-1} is not clearly visible in sample C but is seen in sample G in which the water absorption was much stronger. Liquid water is known to have a band at 2135 cm^{-1}. In fact, the spectrum of ThF_4 bears a striking resemblence to the spectrum of liquid water,[13] including the relative intensities of the three water bands centered at 3390, 2135 and 1640 cm^{-1}. Willingham, et al.[5] had one ThF_4 film with significantly less water absorption than shown in Figure 7, even when the different ATR parameters are taken into account.

In another sample NN we have measured both the transmittance (T) and ATR spectra, concentrating on the low-frequency line at 1620 cm^{-1}. The transmittance must be analyzed with a three-layer model in which the multiple-reflection effects are averaged properly.[20,21] The transmittance through the 0.18 cm width of the trapezoid with two films was 0.991 that of a coated trapezoid with non-absorbing films. This small deviation from unity had to be determined by x10 scale expansion. For transmittance the calculated peak absorption coefficient was 10 cm^{-1} (assuming the water was uniformly distributed throughout the film). The unpolarized ATR for the coated trapezoid was found to be 0.352 for 25 reflections down the trapezoid at $\theta_t = 48^o$ and 13 reflections back at $\theta_t = 65^o$. Since the instrumental polarization was small for this wavelength, the light was basically

unpolarized. The ATR absorption coefficient was 19 cm^{-1}. Considering the uncertainties in film thickness and difficulties in measuring such a small change in transmittance, and fixing the background level, we find this agreement to be satisfactory. The absorption coefficient for this line in trapezoid C in Figure 7 would be 7 cm^{-1}. It is easier to measure the change in ATR resulting from this absorption than it is to measure the change in T. By extrapolating, we estimate that we can easily measure an ATR of 0.99 (with x10 scale expansion) which for a film 4.1 μm thick would be produced by an absorption coefficient of 0.2 cm^{-1}. More sophisticated techniques such as a cold photoconducting detector and data processing by averaging many spectra should permit measuring an ATR = 0.999 and thus an α = 0.02 cm^{-1}. We usually measure the peak absorption coefficient in a vibration band, and we must be able to estimate where the background ATR level is with no absorption.

We have noticed that the strong band at 3400 cm^{-1} which gives ATR = 0.5 for trapezoid C in Figure 7 can be even larger in some samples (G) with ATR < 0.01. We see no reason, once the first couple of monolayers are formed, for further physisorption to be very sensitive to the absorbate, although it may be sensitive to the orientation of the molecules in the first monolayer. This suggests a large amount of the water is in the film rather than on the surface, because water in physisorbed layers typically gives only a few percent absorptance in an uncoated CaF_2 trapezoid. Therefore, in an attempt to determine the location of the water, we placed the ThF_4/CaF_2 sample into an UHV system and single passed it. The ATR before pumping was 0.46 while the double-pass ATR of Figure 7 was approximately 0.5 may be due to a different optical system for the vacuum experiments in which there was considerable polarization. We could not completely plane polarize due to lack of signal. Another reason may be a dependence of the water content of the film on the relative humidity of the air surrounding the film. After evaluation for 0.5 hr to 1 x 10^{-7} Torr, the ATR rose to ~ 0.53. After pumping for 17 hr to 1 x 10^{-8} Torr, the ATR rose to ~ 0.58. After baking the UHV chamber for 25 hr at 200°C, the ATR rose to ~ 0.79 with the pressure at 2 x 10^{-9} Torr. When

distilled water was admitted into the chamber, the ATR dropped quickly in 1 min and then more slowly for another 30 min reaching 0.51. The data indicate that further slight decrease in ATR would have occurred if we had waited for hours. Were the absorption due to a surface layer of water on the ThF_4, the value of $R^{25} = 0.46$ would be equivalent to a 66Å layer of water. We find this hard to believe, since our work on Si, CaF_2, GaAs and ZnSe all suggest thin layers of water in equilibrium with air. It is more reasonable to assume that this much water is distributed throughout a substantial portion of the film in cracks or on polycrystalline granules. Measurements on trapezoid G showed absorptance was > 0.99 or $R^{25} < 0.01$, which corresponds to an equivalent water layer > 425Å thick. Since both trapezoids G and C had ThF_4 films of comparable thickness, this suggests that the water is contained in the films rather than on the surface, since we would not expect the ThF_4 surfaces themselves to adsorb water very differently. Water may have been absent from the film during its preparation in the evaporation bell jar and only have entered the film when it was exposed to the air. We did not pump and bake the sample for days, so we cannot infer whether or not all of the water is removable. This behavior implies that the film, as grown, is porous to water at least near the surface, and that to eliminate the absorption at 3400 cm^{-1} will require preparing a denser film. Obviously, some water may still adsorb to the surface of the ThF_4. Our measurements of ThF_4/CaF_2 are summarized in Table 1 by a listing of the absorption coefficient due to water at 3400 cm^{-1} as obtained from the ATR and/or T analysis. It appears that lower absorption is obtained with higher substrate temperature except for the anomalous behavior of sample C. While samples C and G were grown under similar conditions as far as the parameters in Table 1 indicate, the absorption is greatly different. Sample C looks out of place as far as trends are concerned. In any case the magnitude of absorption for all samples is clearly much too high for the films to be useful at HF laser frequencies.

Thus, there is a somewhat thinner water layer on ZnSe than on CaF_2. This calculation utilizes a model consisting of a CaF_2 substrate, a ZnSe film and a thin water film. This value depends on where the background is placed, but this cannot be determined by comparison with an uncoated CaF_2 trapezoid, since water absorptance on CaF_2 (~6.5%) is stronger than on ZnSe (<3%).

ATR measurements on bulk ZnSe trapezoids[5] reveal weak absorption due to water at 3400 cm^{-1}. We estimate from several spectra <2% absorptance for 25 reflections at $\theta = 45^{o}$. This corresponds to a water film of ~ 3.5Å. This calculation utilizes a model consisting of a ZnSe substrate and a thin water film. It is curious to note that for the first model, a 2.5Å film gives 3% absorptance, while for the second model, a 3.5Å film gives 2% absorptance. This is due, in part, to the different number of reflections but primarily due to the fact that the ZnSe film produces interference effects.

There is considerable uncertainty in choosing the background level to determine absorptance. Also, the different relative humidities for the two types of ZnSe samples, film and trapezoid, as measured by different investigators on different days in different laboratories may cause different amounts of water adsorption. In view of these two uncertainties, we conclude that the water-film thickness on both the ZnSe film and ZnSe trapezoid are comparable, ~3Å, and that the film itself is free of water for sample H. This is not the case for sample F, for example, and we conclude here that the film contains large amounts of water in addition to having an adsorbed water layer on its surface.

The spectrum in Figure 8 for sample M was obtained with unpolarized light. In addition to the sharp line absorption, there are some subtle oscillations which we investigated further. These "fringes" were somewhat stronger in s- than in p-polarization. We also measured the normal-incidence transmittance through the thin dimension of the trapezoid. Interference fringes were observed with maxima at 3950, 3570, 3170, 2750 and 2340 cm^{-1} and minima in between. These transmission fringes were nearly 180^{o} out of phase with the ATR "fringes."

C. $ZnSe/CaF_2$

ZnSe films deposited on CaF_2 have also been studied. In Figure 8 are shown p-polarized (sample II) and unpolarized (sample M), double-pass ATR spectra. The ZnSe film on CaF_2 seemed to scatter light more strongly than the uncoated trapezoid of Figure 2. There is a characteristic, but very weak, absorption band at 3400 cm^{-1} probably due to H_2O. The three usual CH bands near 2920 cm^{-1} are present. There are sharp bands at 3393, 1530, 1460 and 1390 cm^{-1} of unknown origin. Since plasma cleaning caused the three CH bands near 2920 cm^{-1} and the three bands near 1460 cm^{-1} to largely disappear, we conclude that these were caused by surface contaminants. The sharp band at 3393 cm^{-1} remained, however, and it has not been identified. The three bands near 1460 cm^{-1} were not seen in ThF_4/CaF_2 samples and were probably not caused by the same hydrocarbons which produced the 2920 cm^{-1} CH bands. As in Figure 3, a band at 1733 cm^{-1} was present when the 2920 cm^{-1} CH bands were strong, but absent when they were weak (on all surfaces: CaF_2, ThF_4 and ZnSe).

The water absorption near 3400 cm^{-1} varied considerable from sample to sample with films grown at low temperatures generally showing more absorption than films grown at high temperatures. In Table 1 we give values of film absorption coefficient calculated assuming that the water is uniformly distributed throughout the film. Samples, M, L, F, grown at room temperature or 120°C, show significantly less absorption.

The amount of H_2O absorptance at 3400 cm^{-1} was very small in sample H. We estimate < 3% absorptance, and from analysis of the ATR spectrum the peak absorption coefficient was < 1 cm^{-1}. The reduction of water absorption suggests that the 4Å layer was removed from the CaF_2 surface in the evaporation process as the ZnSe was deposited or when the substrate was heated. The film essentially "encapsulates" the CaF_2 surface protecting it from atmospheric water. The small amount of water in Figure 8 is then either in the film, at the CaF_2 surface, or at the ZnSe surface. If it is adsorbed on the ZnSe surface, 3% absorptance corresponds to a water layer 2.5Å thick.

Thus, there is a somewhat thinner water layer on ZnSe than on CaF_2. This calculation utilizes a model consisting of a CaF_2 substrate, a ZnSe film and a thin water film. This value depends on where the background is placed, but this cannot be determined by comparison with an uncoated CaF_2 trapezoid, since water absorptance on CaF_2 (~6.5%) is stronger than on ZnSe (<3%).

ATR measurements on bulk ZnSe trapezoids[5] reveal weak absorption due to water at 3400 cm^{-1}. We estimate from several spectra <2% absorptance for 25 reflections at $\theta = 45^{o}$. This corresponds to a water film of ~3.5Å. This calculation utilizes a model consisting of a ZnSe substrate and a thin water film. It is curious to note that for the first model, a 2.5Å film gives 3% absorptance, while for the second model, a 3.5Å film gives 2% absorptance. This is due, in part, to the different number of reflections but primarily due to the fact that the ZnSe film produces interference effects.

There is considerable uncertainty in choosing the background level to determine absorptance. Also, the different relative humidities for the two types of ZnSe samples, film and trapezoid, as measured by different investigators on different days in different laboratories may cause different amounts of water adsorption. In view of these two uncertainties, we conclude that the water-film thickness on both the ZnSe film and ZnSe trapezoid are comparable, ~3Å, and that the film itself is free of water for sample H. This is not the case for sample F, for example, and we conclude here that the film contains large amounts of water in addition to having an adsorbed water layer on its surface.

The spectrum in Figure 8 for sample M was obtained with unpolarized light. In addition to the sharp line absorption, there are some subtle oscillations which we investigated further. These "fringes" were somewhat stronger in s- than in p-polarization. We also measured the normal-incidence transmittance through the thin dimension of the trapezoid. Interference fringes were observed with maxima at 3950, 3570, 3170, 2750 and 2340 cm^{-1} and minima in between. These transmission fringes were nearly 180^{o} out of phase with the ATR "fringes." We recently calculated[6] that ATR interference fringes may

be observable for the case of a large-index film on a low index substrate if the film is somewhat absorbing. Of course, ATR fringes are not visible if the film is lossless. The "fringes" observed here fit the calculated results that s-polarization fringes are stronger than p-polarization fringes, and the fringe pattern is roughly out of phase with the transmission fringe pattern. However, the fringe spacing for each set of fringes should be slightly different due to the angle effect in ATR, and we cannot detect this slight difference although calculations indicate it should be observable.

($\Delta\omega_T$ = 400 cm^{-1}, $\Delta\omega_{ATR}$ = 430 cm^{-1} for $\theta_t = 48^o$).

In addition, a detailed calculation for the double-pass trapezoid (assuming a uniform absorption coefficient over the spectral range) indicates that the fringes due to the down pass have a spacing somewhat different from the fringes due to the return pass, implying that the total ATR fringe pattern should be more complicated than it actually appears. Interestingly, the maximum to minimum ration $(1 - R_{MAX})/(1 - R_{MIN})$ for ATR fringes is independent of magnitude of absorption coefficient, so we can assume any small convenient value to calculate fringe shape and position. We also established that the ATR "fringes" were not due to an accidental ZnSe coating on the end faces.

Calculations indicate that a finite absorption coefficient is needed to produce ATR fringes. However, scattering due to rough surfaces at the CaF_2/ZnSe interface and the ZnSe/air interface may be equivalent to absorption in that it reduces the amplitudes of multiply reflected rays. This may be the origin of the observed ATR "fringes", since the surface quality indicated scattering to the eye. At the moment we cannot clearly demonstrate the presence of ATR fringes in sample M. We did see less distinct oscillations in some of the other ZnSe/CaF_2 samples but not in sample H in Figure 8, for example.

CONCLUSIONS AND SUMMARY

The preparation and infrared characterization of thin films of ZnSe and ThF_4 on CaF_2 by internal-reflection spectroscopy is described. These are useful as high- and low-index films for antireflection coatings in the 3-4 μm region. A number of useful procedures and

techniques are given which are applicable to other substrates, coating materials, and wavelengths.

Both the substrate surface absorption and the thin-film absorption have been studied. Qualitative examination of the internal-reflection spectra on specially designed substrate trapezoids indicates the presence of H_2O and hydrocarbons which have detectable absorption in the 2.5 to 4 μm regions in which HF and DF lasers operate. These results are in accord with previous observations elsewhere. In this present work, the absorption coefficients were estimated. This has involved consideration of the general case of films having indices both higher and lower than that of the substrate. This differs from the usual case of attenuated total reflection, where low-index films on high-index substrates are treated in either a thin- or thick-film approximation.

An attempt was made to estimate the thickness of the water and hydrocarbon layers needed to account for the observed absorptance and to determine the location of this absorption, i.e., whether it is due to adsorbed molecules on the surface or distributed within the film. In the case of a clean CaF_2 surface exposed to saturated water vapor, the water absorption appears due to a chemisorbed layer of water about 3 Å thick and a physisorbed layer about 10 Å thick. In the case of a "dirty" CaF_2 surface in air, the absorption appears due to a layer of water about 4 Å thick. This is sufficiently small so that a surface location of the impurity seems reasonable. On the other hand, to account for the water absorption in ThF_4 films would require assuming an adsorbed water film much thicker which varied markedly from sample to sample. Since this is not reasonable, the alternative is that water is distributed within the pores of the film. Presumably, the water comes from atmospheric contamination after the film is removed from the evaporator. In contrast, ZnSe films appear to manifest much weaker water absorption bands. Analysis of the data for samples prepared at higher temperatures indicate that the absorption was due primarily to an adsorbed water layer on the ZnSe film. The water film adsorbed to both CaF_2 and ZnSe are found to be comparable.

Other evidence concerning the location of the water and hydrocarbon impurities stems from attempts to remove them. The hydrocarbon impurities can be removed by cleaning, but return within hours after exposure to air. However, the saturation time for ThF_4 films is much greater than for CaF_2 surfaces as it may take a longer time for the hydrocarbons to diffuse into the film pores. The return of hydrocarbons to the surface appears to be a two-step process with one stage occurring within minutes and a second stage within hours.

While most of the hydrocarbons can be removed by simple cleaning, water can only be removed nearly completely from surfaces by heating in vacuum. The return of water to surfaces and films appears to be extremely rapid. These results suggest that water absorption by the low-index ThF_4 film might be avoided by deposition of a sealing layer (such as ZnSe) without breaking vacuum. The efficacy of such a procedure could be demonstrated using internal-reflection spectroscopy, and it is hoped to do so in the future.

ACKNOWLEDGMENTS

Fruitful discussion of the adsorption of hydrocarbons and water on CaF_2 surfaces were held with P. H. Klein. J. N. Harrick provided useful information on ATR techniques. This work was supported by ONR and by DARPA.

Table 1. Summary of Film Deposition and Optical Measurements. The thicknesses given in parentheses are calculated from transmission IR interference fringes assuming the two films are of equal thickness.

Trapezoid Letter Designation	Material	Rate Å/min		Thickness μm		Temperature °C	Comments	Optical Measurement	Film Absorption Coefficient at 3400 cm^{-1}	
		Side 1	Side 2	Side 1	Side 2					
K	ThF_4	1560	6470	3.7	2.9	Room		ATR, T		1520
C		6380		4.3	3.9	150	Evaporation Source Exploded	ATR	17	
G		6180	6180	4.3	4.7	160		ATR, T		750
GG		2140	6700	6.6	7.0	200		ATR	~100	
KK		5360	3020	4.0	4.0	200		T		27
NN		3090	970	4.3	4.3	250		ATR, T	31	15
S		7910	2080	3.9	3.9	250	HRL Material	ATR	25	
M	ZnSe	1980	3600	4.9	5.3	Room		ATR, T	2.5	
L				12.0	17.5	120	60 min/side	ATR, T	5.7	
F				(13.1)	(13.1)	120	35 min/side evaporation, cleavage	ATR, T	3.3	
O		1550	1730	5.2	4.9	200		T		
Q		1200	1200	4.9	5.3	200		ATR, T	0.6	
H		4200		(5.6)	(5.6)	200		ATR, T	0.8	
PP		1380	3940	4.1	4.3	250	Re-evaporation, cleavage	T		

References

1. M. Sparks, "Materials for High-Power Window and Mirror Coatings and Multi-layer-Dielectric Reflectors," in NBS Special Publication 462, Laser Induced Damage in Optical Materials 1976, p. 203-213.

2. T. F. Deutsch, "Laser Window Materials - An Overview," J. Electr. Mat. 4, 663-719 (1975).

3. N. J. Harrick, Internal Reflection Spectroscopy (Wiley, New York, 1967).

4. T. F. Deutsch and R. I. Rudko, Research in Optical Materials and Structures for High-Power Lasers, Final Technical Report Jan. 1973. Contract No. DAAH01-72-C-0719. ARPA.

5. C. Willingham, D. Bua, H. Statz and F. Horrigan, Laser Window Studies, Final Technical Report, Aug. 1975; Contract No. DAAH01-74-C-0719. ARPA.

6. R. T. Holm and E. D. Palik, "Thin-Film Coating Evaluation by Attenuated Total Reflection," in NBS Special Publication 462, Laser-Induced Damage in Optical Materials, Dec. 1976, p. 246-249.

7. H. Wolter, "Optik Dunner Schichten," in Handbuch der Physik, Vol.24, edited by S. Flugge (Springer, Berlin, 1956), p. 461-554.

8. J. T. Cox and G. Hass, "Antireflection Coatings for Optical and Infrared Optical Materials," in Physics of Thin Films, Vol. 2, edited by G. Hass (Academic Press, New York, 1964) p. 239.

9. J. E. Rudisill, M. Braunstein and A. I. Braunstein, "OpticalCoatings for High Energy ZnSe Laser Windows," Appl. Opt. 13, 2075-2080 (1974).

10. V. Wang, C. R. Giuliano and B. Garcia, "Single and Multilongitudinal Mode Damage in Multilayer Reflectors at 10.6 m as a Function of Spot Size and Pulse Duration," NBS Special Publication 435 (1975), p. 216-229.

11. P. B. Barracough and P. G. Hall, "Adsorption of Water Vapour by Calcium Fluoride, Barium Fluoride and Lead Fluoride," J. Chem. Soc. Faraday Trans. I 71, 2266-2276 (1975).

12. R. T. Holm and E. D. Palik, "Effects of Mechanical Polishing Damage on the IR Reflectance and Attenuated Total Reflection Spectra of n-type GaAs," J. Vac. Sci. Technol. 13, 889-893 (1976).

13. H. D. Downing and D. Williams, "Optical Constants of Water in the Infrared," J. Geophysical Research 80, 1656-1661 (1975).

14. J. W. Gibson, R. T. Holm and E. D. Palik, "Hydroxyl and Hydrocarbon Adsorption Effects on CaF_2 Surfaces," Abstract, Bull. Amer. Phys. Soc. 22, 295 (1977).

15. M. Hass and J. A. Harrington, private communication.

16. F. A. Horrigan and T. F. Deutsch, "Research in Optical Materials and Structures for High-Power Lasers, "Final Technical Report, Contract No. DAAH01-70-C-1251 ARPA, Sept. 1971, p. 82.

17. A. Hordvik and L. Skolnik, "Surface and Bulk Absorption in HF/DF Laser Window Materials," See Abstracts for 1976 Topical Meeting on Optical Phenomena in Infrared Materials, Dec. 1-3, Annapolis, Maryland in J. Opt. Soc. Am. 67, 253 (1977).

18. P. Kraatz and S. J. Holmes, "Surface Chemistry and Absorptance of CaF_2 and SrF_2 at DF and CO Wavelengths," see abstracts for 1976 Topical Meeting in Optical Phenomena in Infrared Materials, Dec. 1-3, 1976, Annapolis, Maryland in J. Opt. Soc. Am. 67, 245 (1977).

19. L. H. Little, Infrared Spectra of Adsorbed Species, (Academic Press, New York, 1966), Chap. 10, p. 228.

20. H. E. Bennett and J. M. Bennett, Precision Measurements in Thin Film Optics, in Physics of Thin Films, Vol. 4, edited by G. Hass, M. H. Francombe and R. W. Hoffman (Academic Press, 1967), p. 1-96.

21. C. J. Mogab, "Measurement of Film Thickness from Lattice Absorption Bands," J. Electrochem. Soc. 120, 932-937 (1973).

Figure Captions

1. Schematic diagrams for single- and double-pass trapezoids with definitions of parameters. The "fold out" trapezoids make it simpler to visualize the beam.

2. ATR spectrum of a CaF_2 trapezoid (as received). The absorption bands due to water and hydrocarbons adsorbed to the surface are indicated. The ordinate is adjusted so that 100% reflection corresponds to 0.9. The dashed curve indicates the background if no H_2O or CH absorption were present. The dash-dot curve is the background when the surfaces are polished better to eliminate surface scattering (and H_2O and CH absorption is omitted).

3. Return of absorption due to CH at 2950 cm^{-1} for three different surfaces which are initially cleaned. The solid lines are exponential fits to the data.

4. Calculated ATR (s- and p-polarized) for a polyethylene film on CaF_2 at 2920 cm^{-1} for $\theta = 48^o$ (dotted curves) and 65^o (solid curves). The left ordinate is for N = 1 reflection. The right ordinates are for N = 25 and 13 reflections.

5. Polarization properties of CH absorption bands (a) for the saturation level of Figure 3 for hydrocarbons on CaF_2; (b) for the case of a "dirty" CaF_2 surface.

6. Calculated ATR (s- and p-polarized) for a water film on CaF_2 at 3400 cm^{-1} for $\theta = 48^o$ (dotted curves) and 65^o (solid curves). The left ordinate is for N = 1 reflection. The right ordinates are for N = 25 and 13 reflections.

7. Unpolarized ATR spectra of a ThF_4 films on a CaF_2 trapezoid (samples C and G). Absorption bands due to water and hydrocarbons are indicated.

8. ATR spectra of a ZnSe film on a CaF_2 trapezoid (sample H, p-polarized; sample M, unpolarized).